JACS
JOURNAL OF THE AMERICAN CHEMICAL SOCIETY

Article

pubs.acs.org/JACS

Synthetic Approach To Determine the Effect of Nuclear Spin Distance on Electronic Spin Decoherence

Michael J. Graham,[†] Chung-Jui Yu,[†] Matthew D. Krzyaniak,[†,§] Michael R. Wasielewski,[†,§] and Danna E. Freedman*[,†]

[†]Department of Chemistry and [§]Argonne-Northwestern Solar Energy Research Center, Northwestern University, 2145 Sheridan Road, Evanston, Illinois 60208-3113, United States

Supporting Information

ABSTRACT: Nuclear−electronic interactions are a fundamental phenomenon which impacts fields from magnetic resonance imaging to quantum information processing (QIP). The realization of QIP would transform diverse areas of research including accurate simulation of quantum dynamics and cryptography. One promising candidate for the smallest unit of QIP, a qubit, is electronic spin. Electronic spins in molecules offer significant advantages with regard to QIP, and for the emerging field of quantum sensing. Yet relative to other qubit candidates, they possess shorter superposition lifetimes, known as coherence times or T_2, due to interactions with nuclear spins in the local environment. Designing complexes with sufficiently long values of T_2 requires an understanding of precisely how the position of nuclear spins relative to the electronic spin center affects decoherence. Herein, we report the first synthetic study of the relationship between nuclear spin−electron spin distance and decoherence. Through the synthesis of four vanadyl complexes, $(Ph_4P)_2[VO(C_3H_6S_2)_2]$ (**1**), $(Ph_4P)_2[VO(C_5H_6S_4)_2]$ (**2**), $(Ph_4P)_2[VO(C_7H_6S_6)_2]$ (**3**), and $(Ph_4P)_2[VO(C_9H_6S_8)_2]$ (**4**), we are able to synthetically place a spin-laden propyl moiety at well-defined distances from an electronic spin center by employing a spin-free carbon−sulfur scaffold. We interrogate this series of molecules with pulsed electron paramagnetic resonance (EPR) spectroscopy to determine their coherence times. Our studies demonstrate a sharp jump in T_2 when the average V−H distance is decreased from 6.6(6) to 4.0(4) Å, indicating that spin-active nuclei sufficiently close to the electronic spin center do not contribute to decoherence. These results illustrate the power of synthetic chemistry in elucidating the fundamental mechanisms underlying electronic polarization transfer and provide vital principles for the rational design of long-coherence electronic qubits.

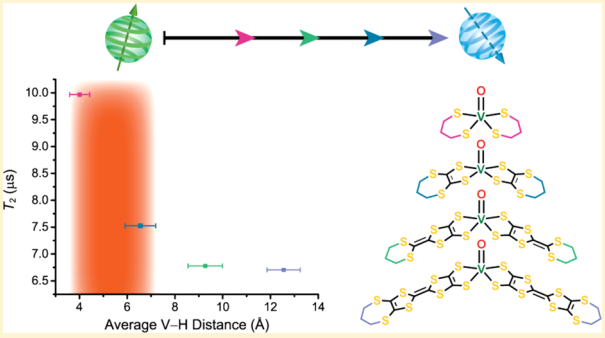

INTRODUCTION

The interplay of electronic and nuclear spins creates unique fingerprints within electronic paramagnetic resonance (EPR) and nuclear magnetic resonance (NMR) spectra. As two illustrative examples, in biological EPR, the interaction between electronic and nuclear spins has been harnessed to provide insight into biochemical processes,[1,2] while in silicon carbide systems, it enables a crucial process known as coherence transfer.[3] Understanding the complex interaction between electronic and nuclear spins could illuminate important processes across a range of fields. Within the realm of electronic−nuclear spin interactions, our interest resides in studying the effect of nuclear spin interactions on electronic spin coherence. Flipping of weakly coupled nuclear spins induces the loss of information stored within electronic spins in a process known as decoherence.[4] There is a paucity of studies probing the effect of nuclear−electronic interspin distance on the characteristic time scale of electronic spin coherence, T_2. Of vital interest to us, creating new knowledge within this area will advance the burgeoning area of electronic spin-based quantum information processing (QIP). QIP is a revolutionary approach to computation which requires long values of T_2.[5−8] Designing complexes that exhibit long coherence times necessitates an understanding of precisely how the position of nuclear spins relative to the electronic spin center affects decoherence. However, the lack of synthetic studies elucidating this positional dependence currently inhibits the rational design of long-coherence complexes.

Of the numerous candidates for qubits, the smallest unit of information in QIP, electronic spin offers considerable advantages, including its inherent quantum nature and ability to be placed into superposition states via the use of pulsed microwaves.[4,9−13] Yet, in comparison with other qubit candidates, electronic spins suffer from short values of T_2. For a quantum object to be viable as a qubit, it must exhibit a T_2 value on the order of 10^4 times the duration of a simple computational operation, which for electronic spin is ∼10 ns.[14] Thus, to be viable, electronic spin qubits require coherence times of >100 μs. Despite a few notable exceptions within

Received: December 19, 2016
Published: February 1, 2017

DOI: 10.1021/jacs.6b13030
J. Am. Chem. Soc. 2017, 139, 3196−3201

molecular and solid-state compounds,[15−22] the vast majority of electronic spin-based qubits exhibit T_2 values in the sub-10-μs regime.[23]

Designing new molecules and materials with long coherence times necessitates a clear set of design principles. Chief among those design principles, as noted above, is the relationship between nuclear−electronic interspin distance and coherence times. While the necessity of understanding this relationship would be obviated by simply removing all nuclear spins from the electronic spin environment, such as in isotopically purified diamond,[24] there are only a limited number of species for which this strategy will be effective.

Creating new design principles requires careful consideration of the impact of nuclear spin on electronic spin coherence. Although nuclear spin diffusion is driven by dipolar coupling between the electron and environmental nuclei, it does not exhibit a simple r^{-3} dependence. Instead, there exists a critical radius, known as the spin diffusion barrier radius, inside of which nuclei are so strongly coupled to the electron spin that they do not undergo flip flops on the experimental time scale, and therefore do not contribute to decoherence.[23] Effectively, the diffusion barrier creates two regimes, within the spin diffusion barrier and significantly distal from electronic spin center, wherein nuclear spins do not shorten T_2. One could therefore envision crafting molecules that, despite containing spin-active nuclei, are designed such that the spin-active nuclei do not contribute to decoherence.

The idea of a diffusion barrier radius (sometimes also referred to as a "frozen core")[25] was first postulated in 1949,[26] and initially observed directly in 1973 via analysis of nuclear relaxation rates of protons near a Yb^{3+} impurity in a crystal of $Y(C_2H_5SO_4)_3{\cdot}9H_2O$.[27] This and other reports on solid-state systems assign the radius as lying between 3 and 10 Å from the metal center.[25,27−30] However, the radius is highly system-dependent, and specific systems such as phosphorus donors in natural-abundance silicon can exhibit radii of upward of 50 Å.[31] Studies of molecular species established a similar range of barrier radii to those of most solid-state systems (between 4 and 10 Å) by methods including time-resolved polarized neutron scattering[32] and fitting T_2 data with a model incorporating a diffusion barrier.[28,33] Notably, thus far, there are no synthetic studies of the diffusion barrier radius. There is, however, ample current research focused on theoretical models of the behavior of nuclear spins in systems exhibiting a barrier radius,[31,34,35] offering promise for the future synergy of theory with our experimental results.

We aimed to address the lack of synthetic studies by designing a series of systems with a range of electron−nuclear distances and examining the effect of that variation on decoherence. Specifically, we targeted a series of coordination complexes based on the $S = {}^1/_2$ vanadium(IV) ion. We selected the V^{4+} species based upon significant previous work demonstrating long coherence times and coherences at temperatures up to room temperature, recommending such species as candidates for rigorous studies of coherence times.[15,36−43] Herein we report the synthesis of a family of four novel vanadium(IV) complexes with a nuclear spin-bearing propyl bridge spaced at controlled distances from the metal center. Within this series, each complex was designed to possess a narrow, discrete range of electron−proton distances. Our results demonstrate that the diffusion barrier radius lies between 4.0(4) and 6.6(6) Å in the studied complexes. This result paves the way for the design of future nuclear spin-containing, long-coherence molecules.

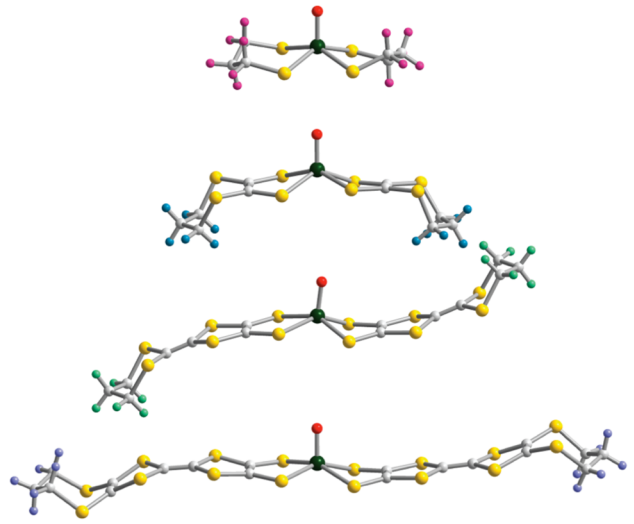

Figure 1. Crystal structures of the anionic complexes of **1**−**4**. Dark green, yellow, red, and gray spheres represent vanadium, sulfur, oxygen, and carbon, respectively. Protons are colored pink in **1**, blue in **2**, light green in **3**, and purple in **4**.

RESULTS AND DISCUSSION

We sought out a series of compounds whereby it would be possible to systematically vary the separation between an electronic spin-bearing metal and a set of nuclear spin-bearing atoms. The vast literature on conjugated carbon−sulfide ligands for organic conductors[44,45] enabled us to identify a series of ligands with which we could accomplish this goal by spacing an alkyl bridge at specific distances from an electronic spin. The nuclear spin-free nature of the carbon−sulfide ligand backbone (98.9% and 99.3% natural abundance of spin-free isotopes for C and S, respectively) and the high modulatory of this chemistry facilitated the rational synthesis of these species. Employing this ligand motif, we synthesized four new vanadium(IV) complexes: $(Ph_4P)_2[VO(C_3H_6S_2)_2]$ (**1**), $(Ph_4P)_2[VO(C_5H_6S_4)_2]$ (**2**), $(Ph_4P)_2[VO(C_7H_6S_6)_2]$ (**3**), and $(Ph_4P)_2[VO(C_9H_6S_8)_2]$ (**4**) (Figure 1). Each complex was carefully designed to house propyl linkers (each containing six protons) at a specific distance from an $S = {}^1/_2$ vanadium(IV) ion (Figure 2). The combination of the improved solubility enabled by the propyl unit relative to species containing the analogous ethyl-bridged ligands,[46] and the propyl moiety's six spin-active protons, recommended it as the nuclear spin-bearing component. Furthermore, the magnitude of the nuclear spin of ^{1}H (μ = 2.79 μ_N for ^{1}H, 99.99% natural abundance) is unusually large relative to other elements on the periodic table, for example, ^{35}Cl (μ = 0.82 μ_N) or ^{14}N (μ = 0.40 μ_N),[47] making it an ideal choice. The aforementioned modularity of the carbon−sulfur scaffold allowed placement of the propyl linkers at well-defined locations, yielding average V−H distances of 4.0(4) Å for **1**, 6.6(6) Å for **2**, 9.3(7) Å for **3**, and 12.6(7) Å for **4**.

The vanadyl coordination complexes were accessed via metalation of the sodium or potassium salt of the appropriate ligand with vanadyl acetylacetonate, followed by cation metathesis with tetraphenylphosphonium bromide. The ligands were synthesized through an approach which relied largely on the $C_3S_5^{2-}$ ("dmit") ligand as a precursor.[48,49] The ligand component of compound **2** was synthesized via nucleophilic attack of the $C_3S_5^{2-}$ moiety on 1,3-dibromopropane,[50] followed by conversion of the thione into a ketone with $Hg(OAc)_2$ to

DOI: 10.1021/jacs.6b13030
J. Am. Chem. Soc. 2017, 139, 3196−3201

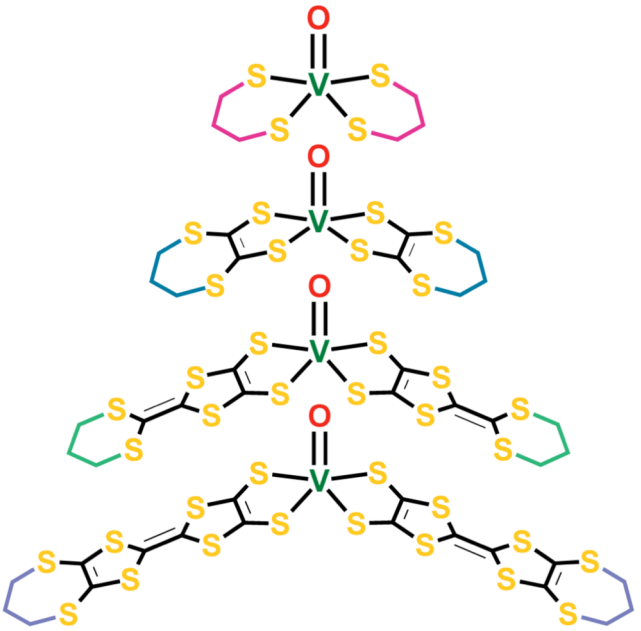

Figure 2. Schematic drawing of the four complexes employed in this study showing the functional components of the ligand design. The electronic spin-bearing vanadium center is highlighted in dark green, while the propyl linker with its six spin-active protons is depicted in variable colors (pink for **1**, blue for **2**, light green for **3**, and purple for **4**).

afford the proligand.[51] The $C_7H_6S_6^{2-}$ ligand for compound **3** involved substituting one of the ketone moieties of thiapendione ($C_4S_4O_2$)[52] for a dibutyltin protecting group, then subjecting that species to a Me_3Al-mediated coupling with an ester containing the 1,3-dithiane moiety to generate the ketone-protected proligand.[53] Finally, we accessed the cyanoethyl-protected proligand of $C_9H_6S_8^{2-}$ via the phosphite-mediated coupling of two C_3S_5-based subunits.[50] For **2** and **3**, ligand deprotection was accomplished via nucleophilic attack of either NaOEt (**2**) or KOMe (**3**) on the ketone moiety, while for **1** and **4**, deprotection occurred via deprotonation (using KOMe in the case of **1** and KO*t*Bu for **4**).

Our initial studies focused on determining the vanadium hyperfine coupling parameter, A, and the electron g-tensor, g, to characterize the magnetic properties of the series of complexes. These compounds were designed to maintain a uniform electronic structure at the spin-bearing center, as significant deviations from that would pose a challenge for deriving meaningful conclusions from the series. Fortunately, previous studies demonstrated that A and g are largely invariant across series of vanadyl complexes[43,54−56] since the orbital bearing the unpaired electron remains constant.[54] To establish the validity of our design approach, we extracted g and A via echo-detected electron paramagnetic resonance (ED-EPR) spectroscopy. ED-EPR results in a spectrum containing the same information as a traditional continuous-wave (cw) EPR spectrum; however, it is recorded as an absorption spectrum instead of the more common derivative line shape.[57] Fitting of the ED-EPR spectra of solutions of **1**−**4** in 45 vol % dimethylformamide-d_7/toluene-d_8 (DMF-d_7/toluene-d_8) to an axial Hamiltonian (see Experimental Details section of the Supporting Information, as well as Table S5 and Figure S1) yielded values of $g_\perp$ = 1.982−1.986, $g_\parallel$ = 1.969−1.978, $A_\perp$ = 120−129 MHz, and $A_\parallel$ = 395−418 MHz, all of which are within the range of values typically exhibited by vanadyl bis(dithiolene) complexes.[40,43,54−56,58,59] These data demonstrate that the complexes possess similar local electronic structures, eliminating variability in electronic structure from consideration.

The performance of a qubit system is described by two figures of merit: the coherence time (T_2), which is the time window of control for the qubit,[8] and the spin−lattice relaxation time (T_1), which serves as an upper limit to T_2, the inverse of which (T_1^{-1}) determines the qubit operating speed.[23,60] Measuring T_1 allows us to determine its impact on T_2 and probe the processes by which spin−lattice relaxation occurs. We therefore performed inversion recovery measurements[57] on dilute solutions of the complexes in 45 vol % DMF-d_7/toluene-d_8 to quantify T_1 (Figure 3, plotted as T_1^{-1}). Examination of the data reveals a high degree of similarity between complexes with values ranging from 11.3(9)−17.5(14) ms at 10 K to 10.32(12)−12.97(13) μs at 140 K. Furthermore, the values of T_1 are virtually identical to those previously reported in a study of vanadyl dithiolene complexes,[43] as are the values obtained by fitting the data to an equation modeling T_1 which incorporates the effect of a direct and a Raman process (see Supporting Information). The direct process is a phonon-mediated spin flip in which the emitted photon is of the exact energy of the spin transition, whereas the two-phonon Raman process works analogously to the Raman scattering of light, where the difference between the energies of the two phonons is equal to the energy of the spin flip.[23] These two processes are commonly assigned as the predominant contributors to T_1 below 100 K.[23,61] The surprising consistency of T_1 values between two families of complexes with significantly different ligand sets speaks to the importance of the immediate coordination sphere around the vanadium ion in influencing T_1 and the relative irrelevance of the composition of more distant elements of the ligand sphere. It also provides further evidence of the uniformity of the series of compounds with regard to every variable except nuclear spin proximity.

Following measurement of T_1, we sought to determine the parameter directly influenced by interactions between electronic and nuclear spins, T_2. Measurement of the coherence times (T_2)

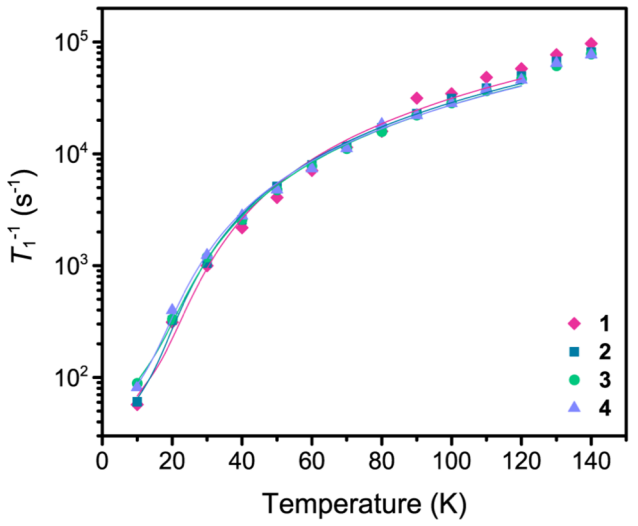

Figure 3. Temperature dependence of T_1^{-1} for **1**−**4** in DMF-d_7/toluene-d_8. Fits of the data to an equation accounting for effects from the direct and Raman processes are shown as lines (see Experimental Details section of Supporting Information for additional details, as well as Tables S6 and S7, and Figure S2).

DOI: 10.1021/jacs.6b13030
J. Am. Chem. Soc. 2017, 139, 3196−3201

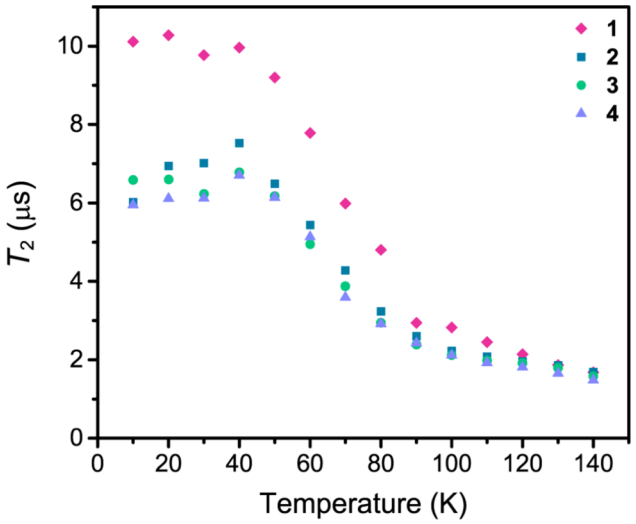

Figure 4. Temperature dependence of T_2 for **1**−**4** in DMF-d_7/toluene-d_8.

of the complexes proceeded via application of a standard Hahn echo pulse sequence[57] at temperatures between 10 and 140 K, and fitting of the resulting decay curve to a stretched exponential function (Figure 4, also Table S8 and Figure S3).[33] All T_2 measurements were acquired in DMF-d_7/toluene-d_8 to minimize the solvent contribution to decoherence, as deuterons possess a significantly lower magnetic moment (μ = 0.86 μ_N) than protons.[47] The most noticeable feature of the data set is the longer T_2 values exhibited by **1** than those of **2**−**4**; at 40 K, **1** possesses a T_2 value of 9.97(3) μs, whereas **2**−**4** exhibit values of 6.70(2)−7.52(2) μs. Upon closer inspection, it is further evident that **2** exhibits slightly longer values of T_2 than **3** and **4** across the range of measured temperatures (e.g., 7.52(2) μs for **2** at 40 K, compared with 6.78(2) μs for **3** and 6.70(2) μs for **4**). The observed differences in T_2 are consistent with a model for decoherence incorporating a nuclear spin diffusion barrier. Specifically, the decrease in T_2 on moving from **1** to **2**, and then to **3** and **4**, is consistent with the protons of **1** being positioned inside the diffusion barrier radius, those of **2** being located close to the barrier radius, and those of **3** and **4** occupying positions significantly outside the barrier radius (Figure 5). This implies a barrier radius of between 4.0(4) and 6.6(6) Å from the spin center (Figure 6). Furthermore, the fact that there is only a minimal change in T_2 on moving from **3** to **4** (9.3(7) and 12.6(7) Å, respectively) potentially suggests that the distance at which nuclei contribute maximally to decoherence is approximately 13 Å. Future work on analogous complexes with greater V−H distances will be necessary to confirm this. Knowledge of the maximal decoherence radius is extremely important for the design of long-coherence complexes, and until now has never been addressed specifically in the literature.

The diffusion barrier, illustrated in Figure 5, defines multiple regions by their differing nuclear−electronic coupling strengths. The nuclear spins closest to the electronic spin lie within the diffusion barrier, and are strongly coupled to the electronic spin, preventing the spin flips that erase information. That portion is depicted in a blue circle. Since the protons of compound **1** occupy positions in this region, the strength of the magnetic coupling between those protons and the electronic spin ties them together, preventing them from contributing to decoherence. The next region of interaction is described by sufficiently weak coupling to prevent the spins from locking, but sufficiently strong coupling to enable the electronic spin to experience the effects of nuclear spin-based decoherence. The protons of compounds **3** and **4** occupy this region, and thus the electronic spins in these compounds experience the maximum impact of decoherence. We postulate that if a complex were designed with a propyl bridge significantly greater than 13 Å from an electronic spin, it would enter the final regime wherein the distal interactions do not engender decoherence.

This hypothesis could be tested by expanding the current data set to additional complexes with longer V−H spacings, and by devising studies to probe the common scenario of baths of nuclear spins. In a spin bath, nuclear spin−nuclear spin interactions and the increase in the number of nuclear spins at a given radius from the qubit center with r^2 both strongly affect the distance−T_2 relationship.[34,35] Performing these studies would shed light onto the generality of these conclusions, and provide insight into the precise end of the diffusion barrier.

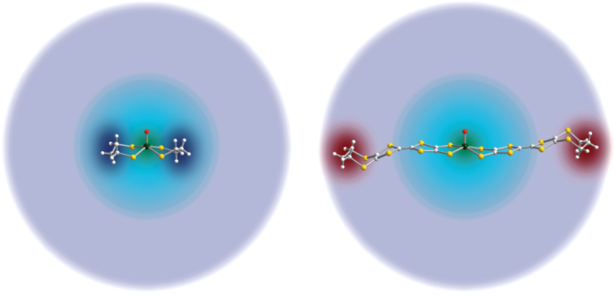

Figure 5. Depiction of our model of the measured diffusion barrier. On both sides, the inner blue circle indicates the diffusion barrier while the larger purple circle indicates the region in which nuclei contribute maximally to decoherence. At the left, the ligand protons are positioned within the diffusion barrier radius and thus do not contribute to decoherence. At the right, the protons are fully outside the barrier radius and contribute significantly to decoherence. Note that although the barrier is not necessarily spherical, we have depicted it as such for simplicity.

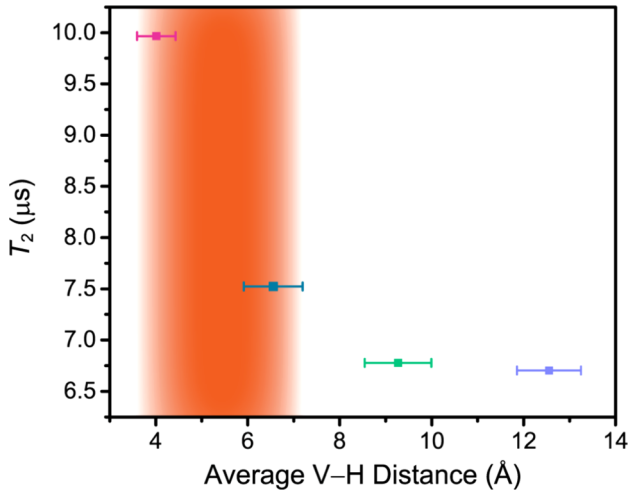

Figure 6. Plot of T_2 versus average V−H distance at 40 K for **1**−**4** in DMF-d_7/toluene-d_8. Horizontal error bars represent the standard deviation for the distribution of V−H distances. Vertical error bars are inside the symbols in all cases. The area highlighted in orange represents the window for the potential extent of the diffusion barrier.

DOI: 10.1021/jacs.6b13030
J. Am. Chem. Soc. 2017, 139, 3196−3201

Thus, the distance dependence of contributions to T_2 remains a fruitful area for future study.

The shape of the temperature dependence of T_2 for the complexes offers further information about the types of processes contributing to decoherence in different temperature regimes. Between 10 and 40 K, the values of T_2 for all species are approximately constant. Decoherence in this regime is dominated by nuclear spin diffusion, as is frequently observed for coordination complexes in spin-bearing solvents.[15,23,62,63] Above 40 K, the drop in T_2 is assigned to the onset of methyl group rotation occurring at a frequency comparable to the experimental time scale. As the temperature further increases above 80 K, the contribution of methyl rotations decreases as the rotational time constant becomes faster than the experimental time scale, resulting in a shallowing of the slope of the T_2 vs temperature curve for all complexes.[23,33,63] However, T_2 for all complexes continues to decrease with increasing temperature, attaining values of 1.485(14)−1.69(2) μs at 140 K. Even at high temperatures, T_2 remains approximately 1 order of magnitude lower than T_1, indicating that it is not T_1-limited.

OUTLOOK

Our synthetic studies establish the nuclear spin diffusion barrier at a radius between 4.0(4) and 6.6(6) Å and suggest the maximal decoherence radius may be at approximately 13 Å. These studies offer promise for the synthesis of new candidate qubits with nuclear spin proximate to electronic spin. Indeed, relaxing a rigid nuclear spin-free design principle will inform our future studies on bimetallic qubit systems. Crucially, beyond qubits, the work described herein may impact a wide range of research fields. One area with the potential for dramatic impact is that of dynamic nuclear polarization nuclear magnetic resonance, (DNP-NMR). Extraordinary signal enhancements are possible with DNP-NMR which have the potential to revolutionize NMR spectroscopy of biological systems.[64] However, the exact method of polarization transfer between electrons and nuclei in DNP-NMR, especially in the context of the spin diffusion barrier, remains a matter of ongoing research,[34,35] which hinders the rational development of improved polarization agents. We anticipate these results will provide insight into the future design of such systems.

Outside of molecular polarization agents and qubits, within solid-state quantum sensors, there is ample work on detecting nuclear spins via electronic spin coherence.[65,66] Establishing a distance dependence between electronic spin coherence and nuclear spin proximity may also aid in developing new quantum sensors, an area at the vanguard of quantum technologies.

ASSOCIATED CONTENT

Supporting Information

The Supporting Information is available free of charge on the ACS Publications website at DOI: 10.1021/jacs.6b13030.

Full experimental details, spectroscopic and crystallographic data (PDF)

CIF for **1** (CIF)

CIF for **2**(CIF)

CIF for **3** (CIF)

CIF for **4** (CIF)

AUTHOR INFORMATION

Corresponding Author

*E-mail: danna.freedman@northwestern.edu

ORCID

Michael R. Wasielewski: 0000-0003-2920-5440

Danna E. Freedman: 0000-0002-2579-8835

Notes

The authors declare no competing financial interest.

ACKNOWLEDGMENTS

We thank Prof. J. Zadrozny and M. Fataftah for helpful conversations, and thank Dr. M. Nilges for experimental assistance. This research was performed with funds from the National Science Foundation for CAREER Award No. CHE-1455017 (M.J.G., C.-J.Y., and D.E.F.) and Award No. CHE-1565925 (M.R.W.). We also acknowledge support from Northwestern University, the State of Illinois, and M.J.G. acknowledges an NSF GRFP fellowship (DGE-1324585).

REFERENCES

(1) Sahu, I. D.; McCarrick, R. M.; Lorigan, G. A. *Biochemistry* **2013**, *52*, 5967−5984.

(2) Spatzal, T.; Aksoyoglu, M.; Zhang, L.; Andrade, S. L. A.; Schleicher, E.; Weber, S.; Rees, D. C.; Einsle, O. *Science* **2011**, *334*, 940.

(3) Falk, A. L.; Klimov, P. V.; Ivády, V.; Szász, K.; Christle, D. J.; Koehl, W. F.; Gali, Á.; Awschalom, D. D. *Phys. Rev. Lett.* **2015**, *114*, 247603.

(4) Winpenny, R. E. P. *Angew. Chem., Int. Ed.* **2008**, *47*, 7992−7994.

(5) Feynman, R. P. *Int. J. Theor. Phys.* **1982**, *21*, 467−488.

(6) Nielsen, M. A.; Chuang, I. L. *Quantum Information and Quantum Computation*, 10th anniversary ed.; Cambridge University Press: Cambridge, 2000.

(7) Stolze, J.; Suter, D. *Quantum Computing: A Short Course from Theory to Experiment*, 2nd ed.; Wiley-VCH Verlag GmbH & Co. KGaA: Weinheim, Germany, 2008.

(8) Ladd, T. D.; Jelezko, F.; Laflamme, R.; Nakamura, Y.; Monroe, C.; O'Brien, J. L. *Nature* **2010**, *464*, 45−53.

(9) Affronte, M.; Troiani, F.; Ghirri, A.; Candini, A.; Evangelisti, M.; Corradini, V.; Carretta, S.; Santini, P.; Amoretti, G.; Tuna, F.; Timco, G.; Winpenny, R. E. P. *J. Phys. D: Appl. Phys.* **2007**, *40*, 2999−3004.

(10) Ardavan, A.; Blundell, S. J. *J. Mater. Chem.* **2009**, *19*, 1754−1760.

(11) Stamp, P. C. E.; Gaita-Ariño, A. *J. Mater. Chem.* **2009**, *19*, 1718−1730.

(12) Troiani, F.; Affronte, M. *Chem. Soc. Rev.* **2011**, *40*, 3119−3129.

(13) Aromí, G.; Aguilà, D.; Gamez, P.; Luis, F.; Roubeau, O. *Chem. Soc. Rev.* **2012**, *41*, 537−546.

(14) DiVincenzo, D. P. *Fortschr. Phys.* **2000**, *48*, 771−783.

(15) Zadrozny, J. M.; Niklas, J.; Poluektov, O. G.; Freedman, D. E. *ACS Cent. Sci.* **2015**, *1*, 488−492.

(16) Takahashi, S.; Hanson, R.; van Tol, J.; Sherwin, M. S.; Awschalom, D. D. *Phys. Rev. Lett.* **2008**, *101*, 047601.

(17) Stanwix, P. L.; Pham, L. M.; Maze, J. R.; Le Sage, D.; Yeung, T. K.; Cappellaro, P.; Hemmer, P. R.; Yacoby, A.; Lukin, M. D.; Walsworth, R. L. *Phys. Rev. B: Condens. Matter Mater. Phys.* **2010**, *82*, 201201.

(18) Koehl, W. F.; Buckley, B. B.; Heremans, F. J.; Calusine, G.; Awschalom, D. D. *Nature* **2011**, *479*, 84−87.

(19) Tyryshkin, A. M.; Lyon, S. A.; Astashkin, A. V.; Raitsimring, A. M. *Phys. Rev. B: Condens. Matter Mater. Phys.* **2003**, *68*, 193207.

(20) Morton, J. J. L.; Tyryshkin, A. M.; Ardavan, A.; Porfyrakis, K.; Lyon, S. A.; Briggs, G. A. D. *J. Chem. Phys.* **2006**, *124*, 014508.

(21) Morton, J. J. L.; Tyryshkin, A. M.; Ardavan, A.; Porfyrakis, K.; Lyon, S. A.; Briggs, G. A. D. *Phys. Rev. B: Condens. Matter Mater. Phys.* **2007**, *76*, 085418.

(22) Brown, R. M.; Ito, Y.; Warner, J. H.; Ardavan, A.; Shinohara, H.; Briggs, G. A. D.; Morton, J. J. L. *Phys. Rev. B: Condens. Matter Mater. Phys.* **2010**, *82*, 033410.
(23) Eaton, S. S.; Eaton, G. R. In *Biological Magnetic Resonance*; Berliner, L. J., Eaton, S. S., Eaton, G. R., Eds.; Klewer Academic/Plenum Publishers: New York, 2000; Vol. *19*, Distance Measurements in Biological Systems by EPR, pp 29−154.
(24) Ishikawa, T.; Fu, K.-M. C.; Santori, C.; Acosta, V. M.; Beausoleil, R. G.; Watanabe, H.; Shikata, S.; Itoh, K. M. *Nano Lett.* **2012**, *12*, 2083−2087.
(25) Wald, L. L.; Hahn, E. L.; Lukac, M. *J. Opt. Soc. Am. B* **1992**, *9*, 789−793.
(26) Bloembergen, N. *Physica (Amsterdam)* **1949**, *15*, 386−426.
(27) Wolfe, J. P. *Phys. Rev. Lett.* **1973**, *31*, 907−910.
(28) Milov, A. D.; Salikhov, K. M.; Tsvetkov, Yu. D. *Sov. Phys. Solid State* **1973**, *15*, 802−806.
(29) Hurrell, J. P.; Davies, E. R. *Solid State Commun.* **1971**, *9*, 461−463.
(30) Hansen, A. D. A.; Wolfe, J. P. *Phys. Lett. A* **1978**, *66*, 320−322.
(31) Guichard, R.; Balian, S. J.; Wolfowicz, G.; Mortemousque, P. A.; Monteiro, T. S. *Phys. Rev. B: Condens. Matter Mater. Phys.* **2015**, *91*, 214303.
(32) Stuhrmann, H. B. *J. Optoelectron. Adv. Mater.* **2015**, *17*, 1417−1424.
(33) Zecevic, A.; Eaton, G. R.; Eaton, S. S.; Lindgren, M. *Mol. Phys.* **1998**, *95*, 1255−1263.
(34) Ramanathan, C. *Appl. Magn. Reson.* **2008**, *34*, 409−421.
(35) Smith, A. A.; Corzilius, B.; Barnes, A. B.; Maly, T.; Griffin, R. G. *J. Chem. Phys.* **2012**, *136*, 015101.
(36) Zadrozny, J. M.; Niklas, J.; Poluektov, O. G.; Freedman, D. E. *J. Am. Chem. Soc.* **2014**, *136*, 15841−15844.
(37) Tesi, L.; Lucaccini, E.; Cimatti, I.; Perfetti, M.; Mannini, M.; Atzori, M.; Morra, E.; Chiesa, M.; Caneschi, A.; Sorace, L.; Sessoli, R. *Chem. Sci.* **2016**, *7*, 2074−2083.
(38) Bader, K.; Winkler, M.; van Slageren, J. *Chem. Commun.* **2016**, *52*, 3623−3626.
(39) Tesi, L.; Lunghi, A.; Atzori, M.; Lucaccini, E.; Sorace, L.; Totti, F.; Sessoli, R. *Dalton Trans.* **2016**, *45*, 16635−16642.
(40) Atzori, M.; Morra, E.; Tesi, L.; Albino, A.; Chiesa, M.; Sorace, L.; Sessoli, R. *J. Am. Chem. Soc.* **2016**, *138*, 11234−11244.
(41) Atzori, M.; Tesi, L.; Morra, E.; Chiesa, M.; Sorace, L.; Sessoli, R. *J. Am. Chem. Soc.* **2016**, *138*, 2154−2157.
(42) Bertaina, S.; Gambarelli, S.; Mitra, T.; Tsukerblat, B.; Müller, A.; Barbara, B. *Nature* **2008**, *453*, 203−206.
(43) Yu, C.-J.; Graham, M. J.; Zadrozny, J. M.; Niklas, J.; Krzyaniak, M.; Wasielewski, M. R.; Poluektov, O. G.; Freedman, D. E. *J. Am. Chem. Soc.* **2016**, *138*, 14678−14685.
(44) Coronado, E.; Galán-Mascarós, J. R.; Gómez García, C. J.; Laukhin, V. *Nature* **2000**, *408*, 447−449.
(45) Coronado, E.; Day, P. *Chem. Rev.* **2004**, *104*, 5419−5448.
(46) Kumasaki, M.; Tanaka, H.; Kobayashi, A. *J. Mater. Chem.* **1998**, *8*, 301−307.
(47) *CRC Handbook of Chemistry and Physics*, 97th ed.; Haynes, W. M., Ed.; CRC Press: Boca Raton, FL, 2016; Section 11−2.
(48) Steimecke, G.; Kirmse, R.; Hoyer, E. *Z. Chem.* **1975**, *15*, 28−29.
(49) Hansen, T. K.; Becher, J.; Jørgensen, T.; Varma, K. S.; Khedekar, R.; Cava, M. P. *Org. Synth.* **1996**, *73*, 270.
(50) Kumasaki, M.; Tanaka, H.; Kobayashi, A. *J. Mater. Chem.* **1998**, *8*, 301−307.
(51) Hartke, K.; Kissel, T.; Quante, J.; Matusch, R. *Chem. Ber.* **1980**, *113*, 1898−1906.
(52) Schumaker, R. R.; Lee, V. Y.; Engler, E. M. *J. Org. Chem.* **1984**, *49*, 564−566.
(53) Yamada, J.; Satoki, S.; Mishima, S.; Akashi, N.; Takahashi, K.; Masuda, N.; Nishimoto, Y.; Takasaki, S.; Anzai, H. *J. Org. Chem.* **1996**, *61*, 3987−3995.
(54) Cooney, J. J. A.; Carducci, M. D.; McElhaney, A. E.; Selby, H. D.; Enemark, J. H. *Inorg. Chem.* **2002**, *41*, 7086−7093.
(55) Wenzel, B.; Strauch, P. *Z. Naturforsch., B: J. Chem. Sci.* **1999**, *54*, 165−170.
(56) Kirmse, R.; Dietzsch, W.; Stach, J.; Olk, R. M.; Hoyer, E. *Z. Anorg. Allg. Chem.* **1987**, *548*, 133−140.
(57) Schweiger, A.; Jeschke, G. *Principles of pulse electron paramagnetic resonance*; Oxford University Press: Oxford, 2001.
(58) Wiggins, R. W.; Huffman, J. C.; Christou, G. *J. Chem. Soc., Chem. Commun.* **1983**, 1313−1315.
(59) Collison, D.; Mabbs, F. E.; Temperley, J.; Christou, G.; Huffman, J. C. *J. Chem. Soc., Dalton Trans.* **1988**, 309−314.
(60) Nellutla, S.; Morley, G. W.; van Tol, J.; Pati, M.; Dalal, N. S. *Phys. Rev. B: Condens. Matter Mater. Phys.* **2008**, *78*, 054426.
(61) Zhou, Y.; Bowler, B. E.; Eaton, G. R.; Eaton, S. S. *J. Magn. Reson.* **1999**, *139*, 165−174.
(62) Wedge, C. J.; Timco, G. A.; Spielberg, E. T.; George, R. E.; Tuna, F.; Rigby, S.; McInnes, E. J. L.; Winpenny, R. E. P.; Blundell, S. J.; Ardavan, A. *Phys. Rev. Lett.* **2012**, *108*, 107204.
(63) Eaton, G. R.; Eaton, S. S. *J. Magn. Reson.* **1999**, *136*, 63−68.
(64) Ni, Q. Z.; Daviso, E.; Can, T. V.; Markhasin, E.; Jawla, S. K.; Swager, T. M.; Temkin, R. J.; Herzfeld, J.; Griffin, R. G. *Acc. Chem. Res.* **2013**, *46*, 1933−1941.
(65) Wu, Y.; Jelezko, F.; Plenio, M. B.; Weil, T. *Angew. Chem., Int. Ed.* **2016**, *55*, 6586−6598.
(66) Lovchinsky, I.; Sushkov, A. O.; Urbach, E.; de Leon, N. P.; Choi, S.; De Greve, K.; Evans, R.; Gertner, R.; Bersin, E.; Muller, C.; McGuinness, L.; Jelezko, F.; Walsworth, R. L.; Park, H.; Lukin, M. D. *Science* **2016**, *351*, 836−841.

DOI: 10.1021/jacs.6b13030
J. Am. Chem. Soc. 2017, 139, 3196−3201